Proceedings of the 38th Chinese Control Conference
July 27-30, 2019, Guangzhou, China

A novel shape detection method for continuum soft manipulator based on cable encoders

shuangquan Zou[1], yueyong Lv[1], liqun Zhao[1], guangfu Ma[1], Hao Yan[2]

1. School of Astronautics, Harbin Institute of Technology, Harbin 150001, China
E-mail: a0020924@126.com

2. College of Information Science and Engineering, Northeastern University, Shenyang 110819, China
E-mail: 13644971979@163.com

Abstract: In this paper, a novel shape detecting method is proposed for continuum soft manipulator to detect the shape in real time, so as to achieve high-precision position and attitude control. The method uses three cable encoders to measure the length of the manipulator per section, and they are distributed at 120 degrees apart from the endplate of the manipulator. Based on the theoretical hypothesis that the soft manipulator has infinite degrees of freedom (DOF), the kinematic model for the single-section manipulator is developed by the piecewise constant curvature method. Further, the kinematic model is extended to the multi-section manipulator via improved D-H method, which achieves the mapping from the length information to the pose of the manipulator. Finally, the three-dimensional shape of the soft manipulator is simulated in real time by MATLAB, which verified the effectiveness of the proposed shape detection method.

Key Words: continuum soft manipulator, cable encoder, piecewise constant curvature, improved D-H method, MATLAB

1 Introduction

With the rapid development of automation technology, manipulator has affected people's daily lives in every aspect. Traditional rigid manipulators are used extensively in manufacturing and can be specially programmed to perform a single task efficiently. However, they are operated difficulty in a narrow and unknown environment owing to their rigid joints. Thus, they are no longer able to meet the growing needs of humanity.

The problems mentioned above have been adequately addressed in the soft tissue of biology to replace the rigid joints, such as elephant trunks, tongues and octopus arms. An increasing number of researchers work towards this field, which inspire their interest and make great progress recently [1,2,3,4,5,8]. Researchers have designed and proposed continuum soft manipulator, consisting of a flexible material, like silicone rubber and pneumatic muscles [6], as shown in Fig. 1. The continuum soft manipulator has a continuously deformable structure to deform its shape with soft actuation, and it has infinite degrees of freedom theoretically compared with traditional rigid manipulators. Therefore, it not only shows unexpectedly adaptation, flexibility and sensitivity to conform to unstructured surroundings, but also promises to be able to bend and twist with high curvatures to grasp objects by the whole manipulation. These improved structural characteristics of the soft manipulator make it have broad application prospects in such aspects as industrial production, medical operation, disaster detection, etc [7,9].

Although soft manipulator has the number of advantages that traditional rigid manipulator cannot match, the achievement of soft manipulator proves to be a hard and challenging work. It is challenging to develop accurate kinematic models to successfully describe such soft manipulator, owing to the infinite degrees of freedom in theory. Furthermore, the absence of precise model greatly reduces the control effect of the soft manipulator. According to the automatic control principle, the most direct and effective method to improve the control accuracy is to add a feedback unit to the control system of the soft manipulator to form a closed-loop control system. Therefore, it is necessary to set up a complete and high-precision shape detection system as the feedback unit to detect the three-dimensional shape of the soft manipulator for high-precision control.

To date, a large proportion of researchers have focused on designing and building the shape detection system, and there have been many exciting results. D. Rus [2] uses fiber bragg grating (FBG) sensors inside soft manipulator to detect the shape based on strain measurements. However, there is usually a problem of extendibility and accuracy. Besides, when the soft manipulator bends, the propagation losses of the FBG sensor will occur due to the fragility of optical fibers. Hence, when rising to the critical curvature, the strain measurement is invalid. Another conventional method to detect three-dimensional shape is to take lots of feature points of the soft manipulator by vision [7, 10]. I. Walker [7] tracks each segment of the soft manipulator using the single camera, and calculates its curvature. W. Chao [10] extends the approach to three-dimensional space by using a trinocular camera. In a word, the shape detection system based on vision has a limited range of application, for example, the camera cannot work in a dark and narrow environment.

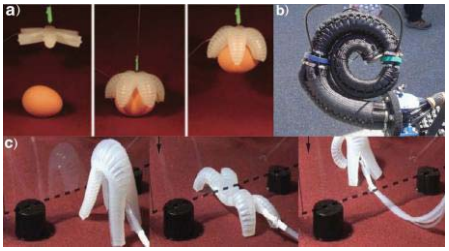

Fig. 1: Several kinds of soft manipulators

*This work is supported by National Natural Science Foundation (NNSF) of China under Grant 61603114 and 61673135.

In this paper, a novel shape detecting method is presented for continuum soft manipulator to detect the shape in real time. Firstly, a distributed sensing network is designed to measure the length of the manipulator based on cable encoders. Secondly, the three-dimensional kinematic model for the single-section manipulator is developed to convert the length information into geometric parameters by the piecewise constant curvature method. Then, we propose the improved D-H method to build the kinematic model for the multi-section manipulator, which finishes the conversion from the geometric parameters to the pose of the manipulator. Finally, the presented shape detection method is simulated by MATLAB, and the prototype experiment is carried out. The simulation results are compared with the experimental results to prove the correctness of the shape detection method.

2 The design of closed-loop control system

The entire closed-loop control system of the soft manipulator consists of three parts, namely the controller, the actuator and the shape detection, as shown in Fig. 2.

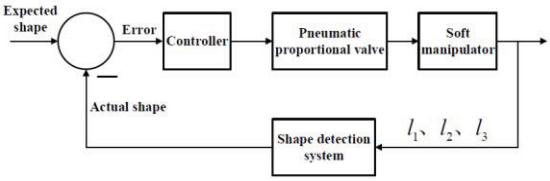

Fig. 2: The structure of the closed-loop control system

2.1 The design of soft manipulator

The soft manipulator, as the actuator in the closed-loop control system, bends and winds the target to achieve the control task.

Nowadays, there are all kinds of soft manipulators. In this work, OctArm [6] continuum manipulator is selected as the research manipulator, i.e., McKibben actuators [6-7], consisting of three closely and evenly distributed pneumatic artificial muscles (PAMs) in each section. Furthermore, three PAMs can extend its length and bend around the x, y and z-axis to obtain the expected 3-D shape when filling each PAM with different pressure. The whole soft manipulator is divided into three sections. Its structural design and prototype is showed respectively in Fig. 3.

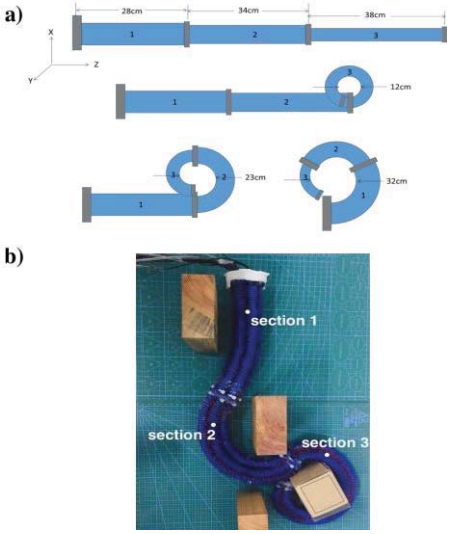

Fig. 3: The structure of the soft manipulator

2.2 The design of distributed sensor network

The shape detection system is the detection unit of the closed-loop control system located in the feedback loop, which measures the actual output of the system and returns to the input. Finally, the soft manipulator is controlled by the error generated by comparing the actual output with the expected input.

In this work, a distributed sensor network is designed to measure the length of the manipulator based on cable encoders. Three cable encoders are distributed at 120 degrees apart from the endplate per section, and one of the cables is attached tightly to the surface of each PAM correspondingly when the PAM expands or contracts, the length of the cable changes accordingly (0.12mm/p). The vertical view of the endplate is shown in Fig. 4. The red and blue circles indicate the cable encoders and the PAMs, respectively.

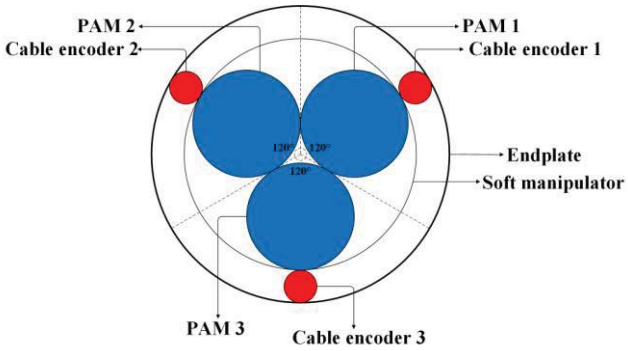

Fig. 4: The distribution of the sensor network

3 Kinematic model

The soft manipulator has no concept of the joint, which is different from the traditional rigid manipulator. It means that the soft manipulator has infinite degrees of freedom theoretically. Therefore, all previous kinematic models of the rigid manipulator have not been applied to the soft manipulator. It is necessary to find a new method to build the kinematic model of the soft manipulator.

3.1 Single-section model

The soft manipulator can be deformed into various shapes in space due to infinite degrees of freedom, resulting in the model to be more difficult to quantify. Therefore, we need to make some ideal assumptions to simplify the structure of the soft manipulator.

When the soft manipulator bents, we consider that the soft manipulator is composed of numerous arcs with different curvatures and different bending planes based on the finite element theory. Thus, the piecewise constant curvature method is proposed to develop the kinematic model of the soft manipulator.

Firstly, for simplicity, the single-section of the soft manipulator is given in Fig. 5 to set up the kinematic model. When the soft manipulator is deformed, the length of the center line remains constant. Therefore, the center line is selected to describe the shape of the soft manipulator for three geometric parameters (the curvature κ_i, the bending plane angle ϕ_i, and the arc length L_i). l_{ij} is defined as the lengths

of the PAM j for the section i, which can be measured through three cable encoders. Where $i \in [1, \mathrm{N}]$ is the section number, $j \in [1,3]$ is the cable encoders number.

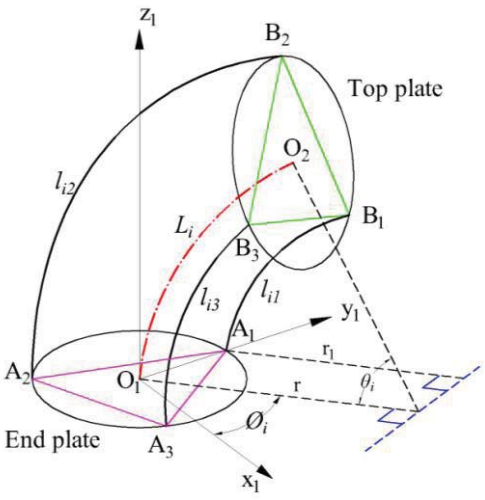

Fig. 5: The single-section model schematic

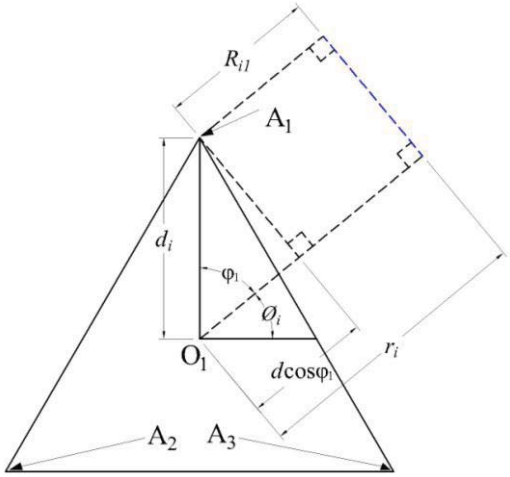

Fig. 6: The vertical view of the endplate

Then, we discuss the expression of three geometric parameters by three length information for a single-section manipulator.

Fig. 6 shows the vertical view of the endplate. R_{ij} is specified as the radius of curvature for the cable encoder j. We can obtain it according to

$$R_{ij} = r_i - d_i \cos\varphi_{ij} \tag{1}$$

Where r is the radius of curvature from the center of the soft manipulator to the center line, d_i is described as the distance from the center of the soft manipulator to each cable encoder, and φ_{ij} is determined as the angle between the plane of the center line and the position of the cable encoder j, where the plane is perpendicular to the endplate.

When both sides of the expression (1) are multiplied by the arc angle θ_i based on $L_i = \theta_i r_i$, it can be rewritten as follows

$$L_i = l_{ij} + \theta_i d_i \cos\varphi_{ij} \tag{2}$$

Through the positional relationship between cable encoder j and the endplate center (shown as Fig.6), the following geometric equations can be derived:

$$\varphi_{i1} = 90^\circ - \phi_i$$
$$\varphi_{i2} = 210^\circ - \phi_i$$
$$\varphi_{i3} = 330^\circ - \phi_i$$
$$\sum_{j=1}^{3} \cos\varphi_{ij} = 0$$

The bending plane angle ϕ_i is the angle between the plane of the center line and the x-axis, where the plane is perpendicular to the endplate. Owing to all the expressions mentioned above, the following equation is satisfied:

$$L_i = (l_{i1} + l_{i2} + l_{i3})/3 \tag{3}$$

Apply the cable encoder 1 and the cable encoder 2 to the expression (2) respectively, and we can obtain $\theta_i d_i = (l_{i2} - l_{i1})/(\cos\varphi_{i1} - \cos\varphi_{i2})$. Above computing process is computed again with PAM2 and PAM3. Further, we derive

$$\phi_i = \tan^{-1}\left(\frac{\sqrt{3}(l_{i2} + l_{i3} - 2l_{i1})}{3(l_{i2} - l_{i3})}\right) \tag{4}$$

As we all known, $\theta_i = \kappa_i L_i = l_{ij}/\mathrm{R}_{ij}$, thus $\mathrm{R}_{ij} = l_{ij}/L_i\kappa_i$, then the equation (1) can be expressed as $\kappa_i = (L_i - l_{ij})/L_i d_i \cos\varphi_{ij}$. Combinned with the equation (3), the expression can be written as $\kappa_i = (l_{i2} + l_{i3} - 2l_{i1})/((l_{i1} + l_{i2} + l_{i3}) d \sin\varphi_{ij})$. Finally, based on the equation (4) and $\sin(\tan^{-1}(y/x)) = y/(\sqrt{x^2 + y^2})$, the curvature κ_i is satisfied:

$$\kappa_i = \frac{2\sqrt{l_{i1}^2 + l_{i2}^2 + l_{i3}^2 - l_{i1}l_{i2} - l_{i1}l_{i3} - l_{i2}l_{i3}}}{d_i(l_{i1} + l_{i2} + l_{i3})} \tag{5}$$

In a word, the equations of the curvature κ_i, the bending plane angle ϕ_i and the arc length L_i can be derived to give the mapping from the length information to geometric parameters. It is mean that we only need to know the three lengths information measured by the cable encoders to calculate three geometric parameters according to above all equations. According to [6], we can obtain the formula (6) to get the position coordinates of the top of the center line P_1 relative to the base coordinate system $\{O_1 - x_1 y_1 z_1\}$, and finally complete the mapping from the geometric parameters to the position coordinates.

$$P_1 = p_1^0 = \begin{bmatrix} \frac{\cos\phi_1(1-\cos\theta_1)}{\kappa_1} & \frac{\sin\phi_1(1-\cos\theta_1)}{\kappa_1} & \frac{\sin\theta_1}{\kappa_1} \end{bmatrix} \tag{6}$$

3.2 Multi-section model

In this section, the presented method for a single-section is extended to a multi-section model (3 sections in this paper) by improved D-H method.

The traditional D-H method describes the spatial relationship of the adjacent two rigid links by 4×4 homogeneous transformation matrix (HTM). Through the sequential transformation, the coordinate of the end actuator relative to the base coordinate system can be finally derived to establish the kinematic model for the multi-section manipulator. Based on the above method, we improve the traditional D-H method combined with the piecewise constant curvature model. It converts the pose of the i+1 section manipulator into the solution of the HTM of the coordinate system between two adjacent section manipulators, as given in Fig. 7. Therefore, the model for the multi-section manipulators can be obtained by multiplying the single-section D-H HTM sequentially.

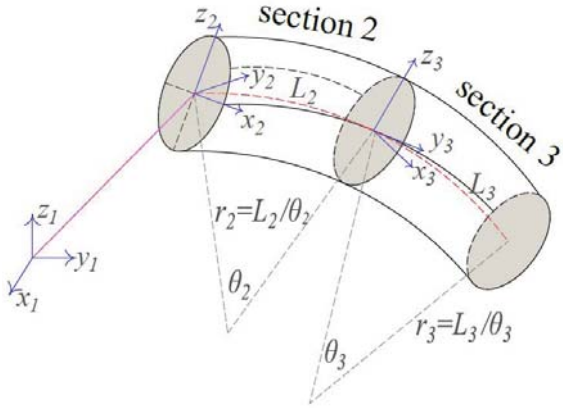

Fig. 7: The multi-section model schematic

According to the geometric analysis, the transformation of the base coordinate system $\{O_1 - x_1y_1z_1\}$ to the coordinate system $\{O_2 - x_2y_2z_2\}$ can be divided into the following steps:

Step1: Rotating around z_1 -axis at ϕ_1;

Step2: Rotating around the new y_1 -axis at $\theta_1/2$;

Step3: Shifting along the new z_1 -axis with $\|O_1O_2\|$;

Step4: Rotating around the new y_1 -axis at $\theta_1/2$;

Step5: Rotating around the new z_1 -axis at $-\phi_1$.

Where $\|O_1O_2\|$ is the length of the vector $\overrightarrow{O_1O_2}$, it can be expressed as follows. The cutaway view of the bending plane for the first section is given in Fig. 8.

$$\|O_1O_2\| = 2r_1\sin(\theta_1/2) \tag{7}$$

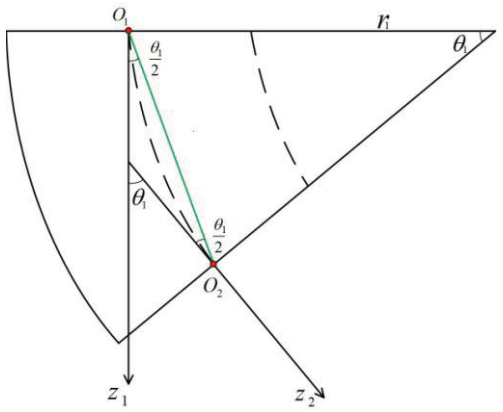

Fig. 8 The cutaway view of bending plane

Hence, the D-H parameters for the first section are shown in table 1.

Table 1: D-H parameters for the first section

sequence	θ	d	a	α
1	ϕ_1	0	0	$-\pi/2$
2	$\theta_1/2$	0	0	$\pi/2$
3	0	$2r_1\sin(\theta_1/2)$	0	$-\pi/2$
4	$\theta_1/2$	0	0	$\pi/2$
5	$-\phi_1$	0	0	0

The HTM from the base coordinate system $\{O_1 - x_1y_1z_1\}$ to the coordinate system $\{O_2 - x_2y_2z_2\}$ can be satisfied by multiplying the transformation matrix sequentially for each step.

$$\begin{aligned} T_2^1 &= Rot(z,\phi_1)Rot(y,\theta_1/2)Trans(z,\|O_1O_2\|) \\ &\quad Rot(y,\theta_1/2)Rot(z,-\phi_1) \\ &= \begin{bmatrix} \cos^2\phi_1(\cos\theta_1-1)+1 & \sin\phi_1\cos\phi_1(\cos\theta_1-1) \\ \sin\phi_1\cos\phi_1(\cos\theta_1-1) & \sin^2\phi_1(\cos\theta_1-1)+1 \\ -\cos\phi_1\sin\theta_1 & -\sin\phi_1\sin\theta_1 \end{bmatrix} \\ &\quad \begin{matrix} \cos\phi_1\sin\theta_1 \\ \sin\phi_1\sin\theta_1 \\ \cos\theta_1 \end{matrix} \end{aligned} \tag{8}$$

We can make the conversion from the base coordinate system $\{O_1 - x_1y_1z_1\}$ to the coordinate system $\{O_2 - x_2y_2z_2\}$, when the T_2^1 is figured out. Apparently, the HTM T_3^2 can be derived to convert the coordinate system $\{O_2 - x_2y_2z_2\}$ to the coordinate system $\{O_3 - x_3y_3z_3\}$ by the same method.

In summary, the HTM T relative to the base coordinate system $\{O_1 - x_1y_1z_1\}$ can be described easily as:

$$T_i = \begin{cases} T_{i+1}^i, & i=1 \\ T_{i-1}T_{i+1}^i, & i>1 \end{cases} \tag{9}$$

Further, the position coordinates of the top of the center line per section relative to the base coordinate system $\{O_1 - x_1 y_1 z_1\}$ are equivalent to

$$P_i = \begin{cases} p_i^{i-1}, & i = 1 \\ P_{i-1} + T_{i-1} p_i^{i-1}, & i > 1 \end{cases} \tag{10}$$

4 Simulation results

In this section, the three-dimensional shape of the soft manipulator is simulated in real time by MATLAB to demonstrate the effectiveness of the proposed shape detection method. When filling the PAMs with pressures, the three-dimensional shape of the soft manipulator will be deformed, and the simulation results will be changed accordingly, matching with the prototype in real time.

For brevity, the simulation is implemented in two cases, namely single-section and multi-section respectively.

4.1 Single-section

The simulation results based on the piecewise constant curvature method for the single-section manipulator are given as follows, including initial state, vertical extension state and bending state.

The simulation results of the initial state for the single-section manipulator are presented in Fig. 9a with no pressure. At this time, $l_{11} = 120.1mm,\ l_{12} = 120.2mm,$ $l_{13} = 120mm$, the prototype is in the state of natural droop in Fig. 9b.

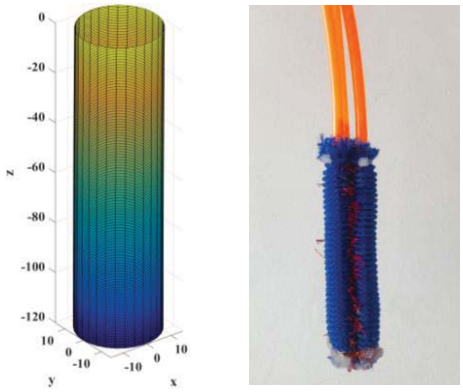

a) Simulation b) Prototype

Fig. 9 Initial state

When $t = 10s$, the same input pressures are filled to three PAMs (presented in Fig. 10b). Because there is no bending deformation, the shape of the simulation is still cylinder in Fig. 10a. However, the cylinder is slender and longer than the initial state due to the increase in pressure. The relationship of geometric parameters still maintains

$$l_{11} = 180mm,\ l_{12} = 179.8mm,\ l_{13} = 180.1mm.$$

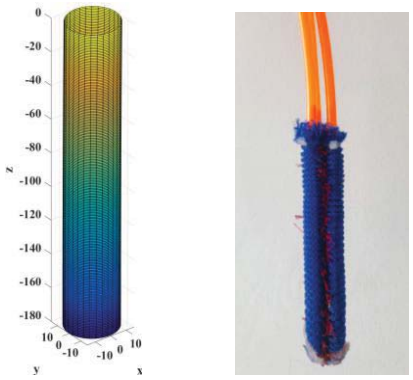

a) Simulation b) Prototype

Fig. 10 Vertical extension state

When $t = 20s$, the bending deformation of the prototype occurs owing to filling different pressures to three PAMs ($p_{PAM3} > p_{PAM1} > p_{PAM2}$). The prototype bends upward, which is consistent with the simulation results in Fig.11. Therefore, geometric parameters satisfy

$$l_{13} = 268mm,\ l_{11} = 235mm,\ l_{12} = 185mm.$$

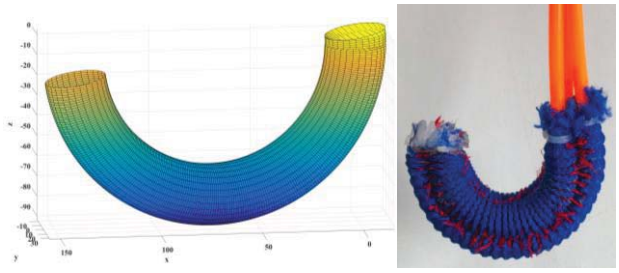

a) Simulation b) Prototype

Fig. 11 Bending state

In summary, it can be seen that the computed parameters and the simulation results agree very well with the experimental results, which completes the verification of the shape detection method. The numerical results of the length during the trial process are shown in Fig. 12.

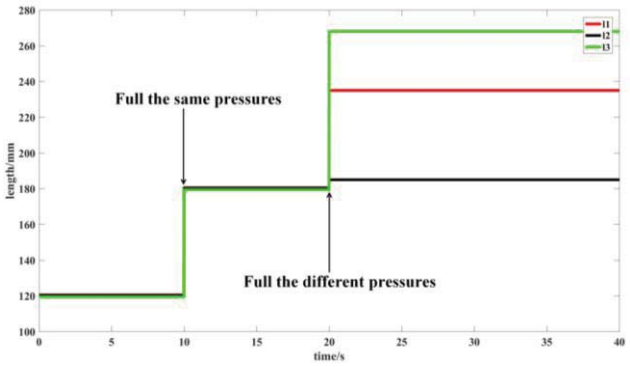

Fig. 12 The numerical results of the length

4.2 Multi-section section

The 3D spatial shape of the multi-section manipulator can also be simulated by MATLAB based on the improved D-H method, including extension state, and bending state.

When three PAMs are full of approximate pressures per section, the multi-section manipulator is in the extended state. The simulation results are presented in Fig.13. The geometric parameters per section can be obtained :

$$l_{11} = 120mm,\ l_{12} = 123mm,\ l_{13} = 124mm,$$
$$l_{21} = 125mm,\ l_{22} = 123mm,\ l_{23} = 121mm,$$

$$l_{31}=126mm,\ l_{32}=124mm,\ l_{33}=125mm.$$

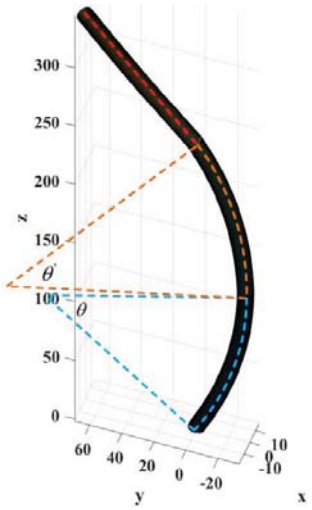

Fig. 13 Simulation result of the extended state

When filling different pressures to three PAMs per section, the multi-section manipulator is in the bending state to wind objects. The simulation results are shown as Fig.14, and the geometric parameters per section are equivalent to

$$l_{11}=121mm,\ l_{12}=123mm,\ l_{13}=125mm,$$
$$l_{21}=236mm,\ l_{22}=187mm,\ l_{23}=269mm,$$
$$l_{31}=236mm,\ l_{32}=186mm,\ l_{33}=268mm.$$

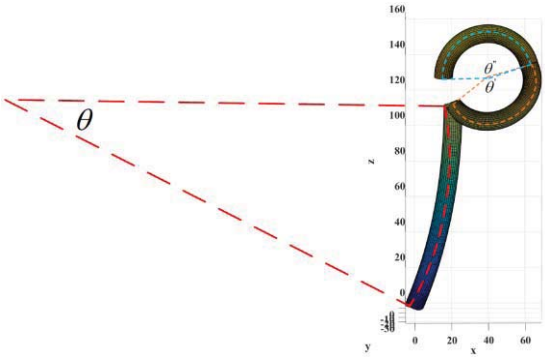

Fig. 14 Simulation result of the bending state

5 Conclusion

An innovative shape detecting approach is proposed for continuum soft manipulator to detect the 3D shape with no delay in this work. A distributed sensing system is established to measure the length of the manipulator based on cable encoders. Then, the kinematic models of the single-section and multi-section soft manipulator are developed respectively. The piecewise constant curvature method for the single-section manipulator is able to convert the length information to geometric parameters. In addition, the coordinates of the center line for the multi-section manipulator can be calculated through the improved D-H method. Finally, the simulation results of the 3D spatial shape for the soft manipulator are obtained in real time by MATLAB, and the validity of the proposed shape detection method is demonstrated by comparing with the prototype.

References

[1] B. Jones, and I. Walker, Kinematics for multisection continuum robots, *IEEE Trans. on Robotics*, 22(1): 43-55, 2006.

[2] D. Rus, Design, fabrication and control of soft robots, *Nature*, 521(7553): 467, 2015.

[3] I. Godage, and D. Branson, Shape function-based kinematics and dynamics for variable length continuum robotic arms, in *Proceedings of Robotics and Automation*, 2011: 452-457.

[4] I. Godage, Dynamics for biomimetic continuum arms: A modal approach, in *Proceedings of Robotics and Biomimetics*, 2011: 104-109.

[5] I. Godage, Modal kinematics for multisection continuum arms, *Bioinspiration & biomimetics,* 10(3): 035002, 2015.

[6] I. Godage, Novel modal approach for kinematics of multi-section continuum arms, in *Proceedings of Intelligent Robots and Systems*, 2011: 1093-1098.

[7] I. Walker, Kinematics and the implementation of an elephant's trunk manipulator and other continuum style robots, *Journal of robotic systems*, 20(2), 45-63, 2003.

[8] M. Grissom, Design and experimental testing of the octarm soft robot manipulator， *Unmanned Systems Technology VIII*, 6230: 62301F, 2006.

[9] M. Aranda , Coordinate-free formation stabilization based on relative position measurements, *Automatica*, 57:11-20, 2015.

[10] W. Chao, Dynamics control of cable-driven silicone soft manipulator, *Shanghai Jiao Tong University*, 1-z, 2015.